JOURNAL OF MATERIALS SCIENCE 28 (1993) 1360–1366

Effect of thickness on ductile fatigue crack propagation in polycarbonate

K. SEHANOBISH
Dow Chemical Company, Freeport, TX 77541, USA
N. HADDAOUI, A. MOET
Department of Macromolecular Science, Case Western Reserve University, Cleveland, OH 44106, USA

Resistance to slow fatigue crack propagation in polycarbonate is investigated with respect to specimen thickness. In the thickness range considered (0.33–3.22 mm), microscopic analysis reveals that a zone of yielded material constitutes the resistance to crack propagation. As the sheet thickness is increased, the amount of yielded material per unit crack surface is reduced. Consequently, faster crack growth rates are observed with increasing specimen thickness. Crack layer theory is applied to analyse crack propagation kinetics and stability. Accordingly, a specific enthalpy of damage (yielding) is found constant for the thickness range considered and is equal to 60 J g^{-1}. It is further noticed that as the thickness increases, resistance to crack initiation increases.

1. Introduction

Crack propagation studies in controlled laboratory conditions can be of considerable value to the design engineer, as well as to the scientist alike, in understanding the mechanism of fracture and in predicting the service life for a pre-existing flaw which may grow to catastrophic failure. However, due to the viscoelastic nature of polymers, the effect of loading conditions, environment, temperature and specimen geometry (particularly thickness) must be assessed.

Poly(bisphenol-A carbonate) (PC) will often deform in a ductile fashion at room temperature [1–6]. A transition to brittle fracture in PC can be observed upon annealing of the polymer below its glass transition temperature [7, 8]. A ductile-to-brittle transition is known to depend on the rate of loading [9], temperature [3, 10, 11] and the thickness of the specimen [3, 10, 12]. For notched specimens of constant thickness, brittle fracture is observed under monotonic loading for sharply notched specimens and fully ductile failure for large notch root radii [3]. Moreover, the resistance to crack growth is markedly decreased at testing temperatures below the room temperature [10, 12]. This effect becomes less prominent with thicker specimens where the rate of crack growth is already high. Also, recent investigations revealed that fatigue crack propagation (FCP) in PC is affected by the molecular weight of the polymer [10, 12]. Resistance to FCP is increased with increase of molecular weight of the material. Fatigue crack propagation in PC is said to be influenced by the loading frequency and cyclic waveform [13], but other studies have suggested otherwise [14]. This discrepancy may be related to the nature and shape of the plastic zone ahead of the crack tip [15]. The initial plastic zone size depends on the shape and the depth of the notch [3]. The shape and size of the transformed zone are determined by the geometry of the notch [3] and the loading level [3, 16].

It is obvious that there are numerous factors that influence the mechanisms involved for a crack and its associated damage to grow to catastrophic failure. However, little attention has been paid to relating the kinetics of FCP to the mechanisms involved. In a previous study [17] of ductile FCP in polycarbonate, it has been noted that the zone of yielded material ahead of the crack tip controls the rate of crack growth. It is the purpose of this study to investigate the effect of thickness on the nature and the extent of the damage zone controlling crack growth. The investigation is carried out utilizing the crack layer methodology developed earlier [17].

2. Experimental procedure

Compression-moulded plaques of Calibre™ 300-3 polycarbonate ($M_w = 35\,000$) were provided by the Dow Chemical Co. with thicknesses ranging from 0.33 to 3.22 mm. Single-edge notched (SEN) fatigue specimens were milled using a sharp fly-cutter at very low speed to the dimensions 120 mm × 20 mm × 0.33 mm. The distance between grips was 80 mm. A 60° V notch of 1 mm depth was milled at the middle of one edge of the specimens. No residual stresses were observed at the notch root of the specimens using a polarized microscope.

Fatigue tests were conducted at room temperature in a laboratory environment on an MTS-800 machine using a constant-amplitude sinusoidal waveform at a frequency of 0.5 Hz. The low frequency is used to

avoid any heat build-up at the crack tip which could influence the subsequent failure. The loading programme was tension–tension with a maximum stress applied at the grips of 33 MPa and a minimum to maximum load ratio of 0.4. The maximum stress was chosen as half of the fracture stress (measured based on cross-sectional area at the grips) of an SEN specimen ruptured under monotonic tensile loading at 50 mm min^{-1}. The crack and the surrounding damage were followed visually from the side using a travelling optical microscope attached to a video camera assembly equipped with a visual display unit from which the history of crack propagation was recorded without interruption of the experiment. Concurrently, load–displacement curves were recorded by means of an X–Y chart recorder. Post-fracture optical observations were carried out with a Zeiss light microscope.

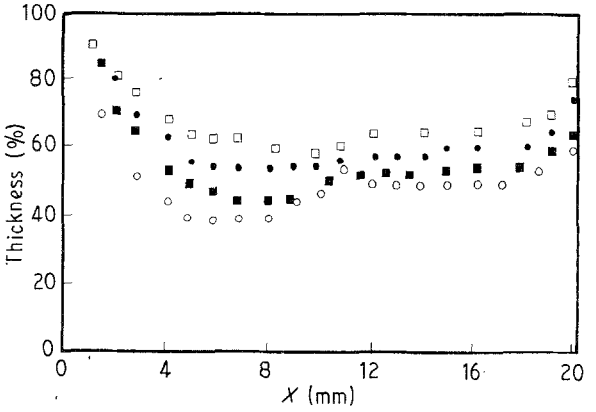

Figure 2 Thickness measurements from the fracture surface across the width of the specimen: X = distance from edge of specimen. Thickness t_0 = (○) 0.33 mm, (■) 0.76 mm, (●) 1.52 mm, (□) 3.22 mm.

3. Results

3.1. Effect of thickness on FCP mechanisms

Fig. 1 is a typical optical micrograph of a side view of a growing crack in a polycarbonate specimen of thickness 3.22 mm. It was seen that the crack layer morphology is essentially the same for all specimens in the thickness range considered. With specimens having a thickness of 4 mm, a mixed mechanism of damage consisting of yielded material and randomly oriented planer brittle microcracks is observed. Since homogeneous yielding is assumed in the current formalism [17], specimens with thickness greater than 3.22 mm are out of the scope of this investigation. Techniques to quantify damage associated with brittle crack propagation in thick polycarbonate sheets are presently sought.

The thickness reduction along the crack path measured from the fracture surface of the broken specimen is shown in Fig. 2. This thinning is taken as a measure of the extent of yielding associated with the crack tip. The data show that the extent of yielding evaluated as the percentage of the original thickness of the specimen follows the same pattern for the thickness range investigated. The extent of yielding is highest at shorter crack lengths and becomes less extensive as the specimen thickness is increased. Consequently, the observed ductile fracture of polycarbonate up to a specimen thickness of 3.22 mm can be treated using the analysis of ductile fracture [17]. It must also be noted that the thickness decreases along the crack path and then increases slightly as the critical crack length (between 10 and 12 mm for all thicknesses) leading to catastrophic failure is approached. The original thickness is gradually recovered as the fast crack propagation occurs to final separation.

3.2. Crack layer characterization

The extension of the yielding along the direction of loading is characterized by the width W of the yielded zone (or active zone) measured at the crack tip when the loading is minimum. (Please note that this width is

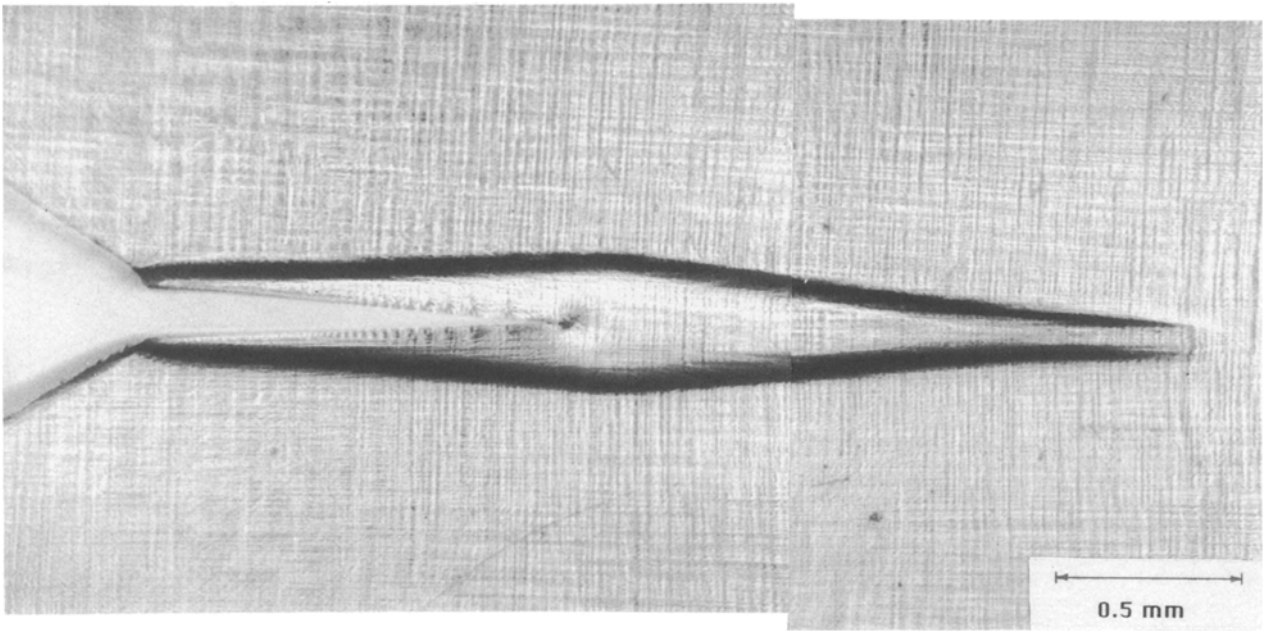

Figure 1 Typical optical micrograph of a growing crack associated with a yielded zone.

measured from the side view of the crack and the active zone.) It reflects the surface-yielded zone, not the core. The data are shown in Fig. 3 where the width is plotted against the crack length. It is evident that the width increases as the crack propagates. More interestingly, it is noted that while the extent of yielding at the crack tip is least in the thickest specimen (Fig. 2), the width of the yielded zone measured from the side is the highest at all crack lengths. In other words, the region under plane stress in a thicker specimen is more prone to plastic deformation. The same conclusion regarding the spread of plasticity at the edge surface can be reached from measurements of the active zone length during crack propagation (Fig. 4).

The width to length ratio of the active zone is plotted in Fig. 5. The increase in width characterizes the expansion of the active zone and the decrease in the aspect ratio demonstrates the distortional process (shape changes) of the active zone that is taking place during active zone translation. A constant value of the active zone width to length ratio of 0.5 corresponds to no shape changes.

Since the width, length and thickness profile can be monitored with the kinetics of crack extension, one could evaluate the volume of yielded material within the active zone and from that the total resistance moment, R_T, is readily estimated as

$$R_T = \frac{\Delta V}{t_0 \Delta a} \tag{1}$$

where ΔV is the volume of the transformed material associated with crack extension from a to $a + \Delta a$, t_0 is

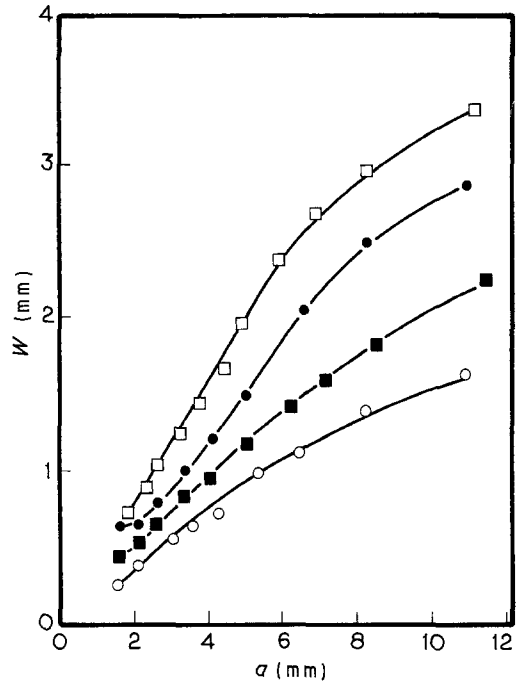

Figure 3 Active zone width W as a function of crack length a. Thickness t_0 = (○) 0.33 mm, (■) 0.76 mm, (●) 1.52 mm, (□) 3.22 mm.

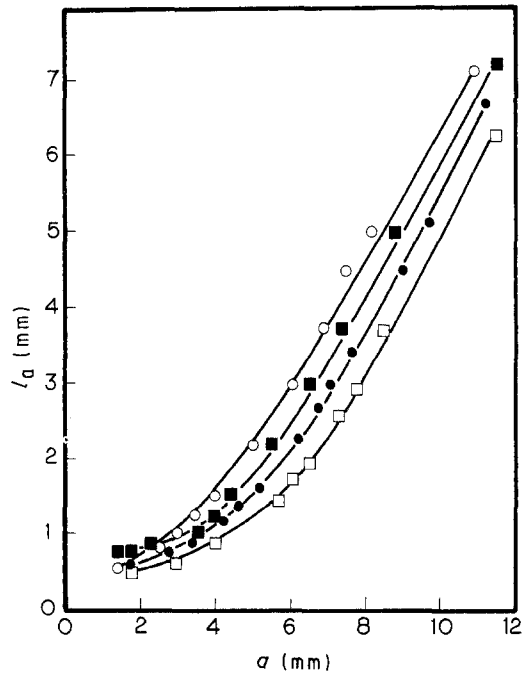

Figure 4 Active zone length l_a as a function of crack length a. Thickness t_0 = (○) 0.33 mm, (■) 0.76 mm, (●) 1.52 mm, (□) 3.22 mm.

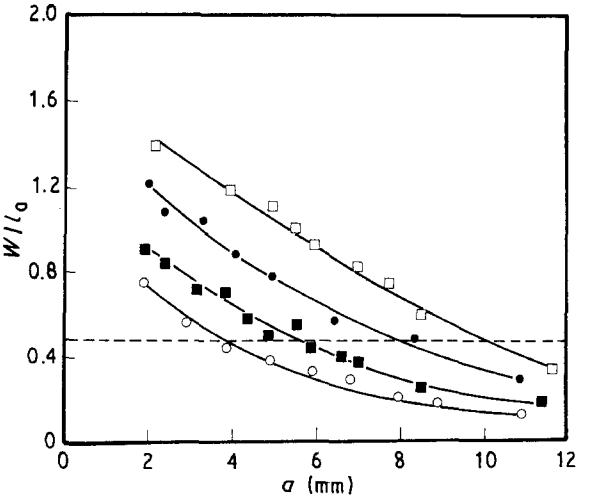

Figure 5 Aspect ratio W/l_a of the active zone as a function of crack length a. Thickness t_0 = (○) 0.33 mm, (■) 0.76 mm, (●) 1.52 mm, (□) 3.22 mm.

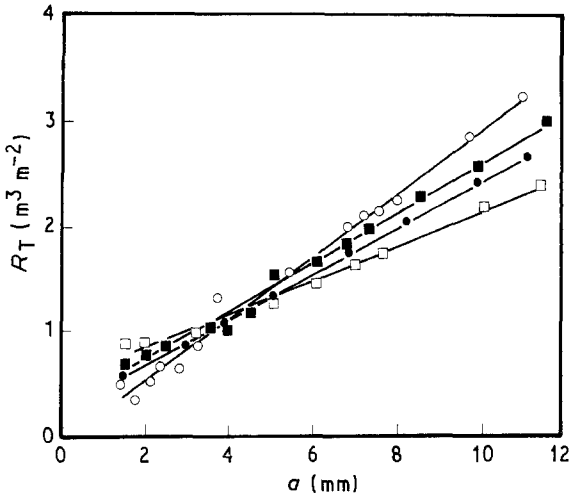

Figure 6 Total resistance moment R_T (amount of yielded material) as a function of crack length a. Thickness t_0 = (○) 0.33 mm, (■) 0.76 mm, (●) 1.52 mm, (□) 3.22 mm.

the initial thickness and Δa is the crack increment. Interestingly, after the damage zone is developed, the resistance to fatigue crack propagation as measured by the total resistance moment increases as the thickness is decreased (Fig. 6). This seems to be due to increasing ductility of the material with the decrease in sheet thickness. It is thought that with the increasing thickness, a state of plane strain becomes prevalent in the vicinity of the crack tip. In plane strain condition, the elastic constant is maximum and thus the spread of plasticity is limited. On the other hand, for a plane stress system in which there is freedom from lateral constraint, a much greater plastic deformation is expected [18].

3.3. Thickness effect on the total energy release rate

The energy released due to propagation of a crack together with the associated damage, A_1, is presented as a function of crack length a in Fig. 7. It should be noted that this change in potential energy encompasses energy release due to crack extension corresponding to the conventional energy release rate J_1, the energy release rate due to expansion of the active zone M, and due to the distortion of the zone N. Accordingly, the quantity measured from load–displacement curves during crack growth under oscillating loads represents the total energy release rate A_1, which may involve all three elementary movements. It is seen in Fig. 7 that the total energy release rate A_1 increases during crack growth of the thickness range, and all curves follow the same trend. However, the rate of increase is lowest at the highest thickness. The conventional energy release rate G is also plotted as a function of crack length to demonstrate the inability of linear elastic fracture mechanics to describe

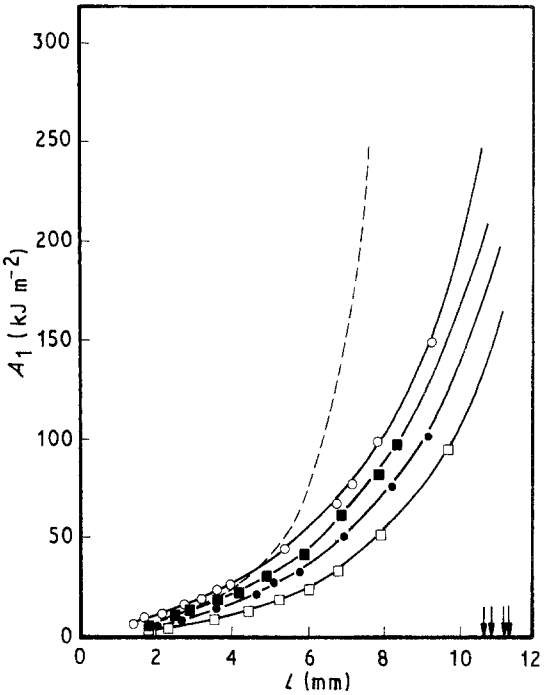

Figure 7 Total energy release rate A_1 as a function of crack length a. Thickness t_0 = (○) 0.33 mm, (■) 0.76 mm, (●) 1.52 mm, (□) 3.22 mm. (---) Conventional energy release rate, G.

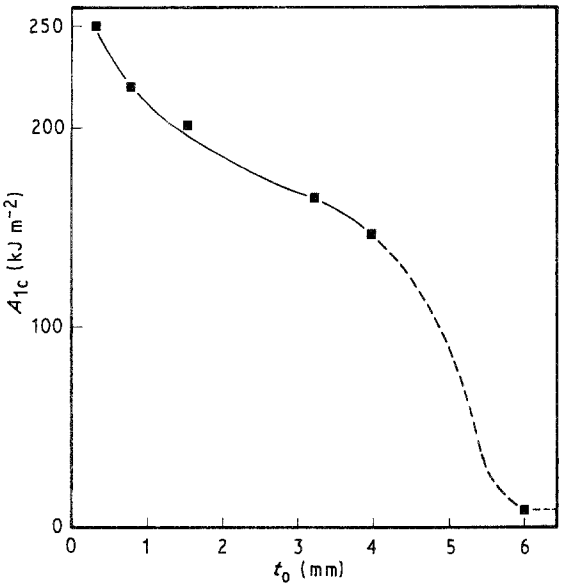

Figure 8 Critical energy release rate A_{1c} as a function of thickness t_0.

such a phenomenon. At critical crack lengths (shown by the arrows in Fig. 7) a transition from slow to catastrophic fracture occurs. The value of A_1 at this crack length is termed the critical energy release rate A_{1c}.

A_{1c} decreases with increasing thickness as shown in Fig. 8 by nearly as much as 50% over the thickness range considered. This indicates a strong thickness effect. This thickness effect on the fracture behaviour of polycarbonate has been previously reported [9]. It was found that 6 mm thick specimens display a mixed mechanism of ductile and brittle behaviour. Specimens of thickness 9 mm, on the other hand, are completely brittle at room temperature [9]. Although this paper only deals with ductile crack propagation, A_{1c} data for 6 mm thick specimens are presented in Fig. 8 for comparison purpose.

4. Discussion

From Fig. 1 it appears that the yielded material is homogeneously transformed. Thus the application of the crack layer formalism developed earlier for ductile polycarbonate fracture is justified [17]. Consequently, the law of crack propagation (active zone translation) may be written as [19, 20]

$$\frac{da}{dN} = \frac{dD/dN}{\gamma^* R_T - A_1} \tag{2}$$

where da/dN is the crack speed, D is the energy dissipated on material transformation within the active zone, γ^* is the specific enthalpy of yielding (material transformation), R_T is the total resistance moment and A_1 is the total energy release rate. Thus the denominator $\gamma^* R_T - A_1$ represents the energy barrier to crack propagation.

4.1. Effect of thickness on the evolution of the energy barrier

Instability of slow crack propagation, i.e. the transition from stable to uncontrolled crack propagation

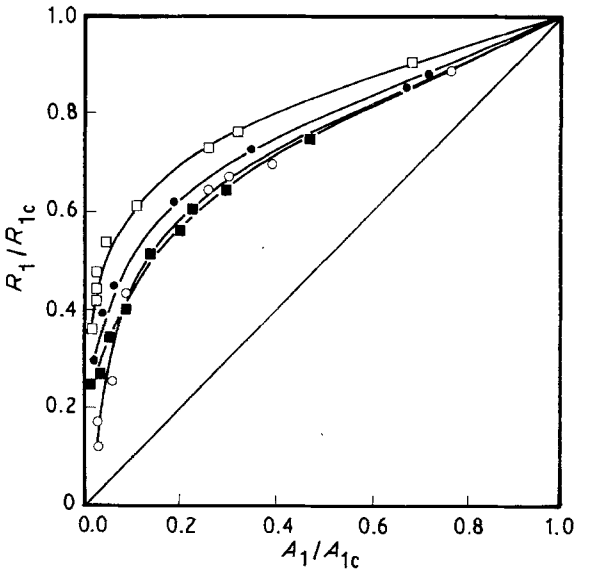

Figure 9 Evolution of total resistance moment R_T as a function of total energy release rate A_1 (normalized with respect to their critical values). Thickness t_0 = (○) 0.33 mm, (■) 0.76 mm, (●) 1.52 mm, (□) 3.22 mm.

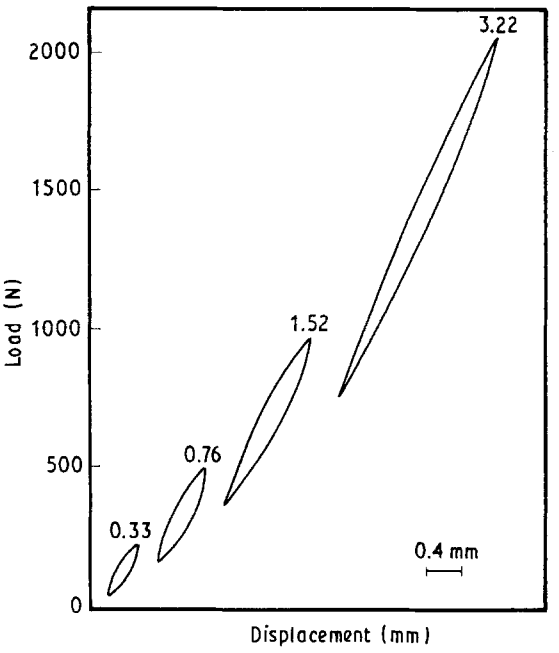

Figure 10 Hysteresis energy at various thicknesses.

occurs when the denominator of Equation 2 vanishes. Therefore

$$A_{1c} = \gamma^* R_{Tc} \tag{3}$$

The subscript c indicates the transition. Replacing $\gamma^* = A_{1c}/R_{Tc}$ in Equation 2 yields

$$\frac{da}{dN} = \frac{dD/dN}{A_{1c}[(R_T/R_{Tc}) - (A_1/A_{1c})]} \tag{4}$$

In crack layer formalism, the total energy release rate is envisioned as the energy available for crack propagation. On the other hand, the energy required is formulated as the product of the specific enthalpy of yielding γ^* and the total resistance moment R_T. The latter expresses the amount of transformed material within the active zone. Value of γ^* for the thickness range considered has been found to be 60 J g^{-1}.

The energy barrier for active zone translation is thus defined as the difference between the energy required and that available for the fracture process. The evolution of this energy barrier normalized by A_{1c} is shown in Fig. 9. The area beneath each curve represents evolution of the energy barrier for a propagating crack. Interestingly, while the critical energy release rate at catastrophic failure is smaller for thicker specimens, the energy barrier expressed by the denominator of Equation 4 decreases with increasing thickness of the specimens.

4.2. Thickness effect on energy dissipation

The crack speed as formulated by Equation 4 is the ratio of the rate of energy spent on damage formation and growth and the energy barrier to crack growth. Since heat exchange measurements between the sample and the surroundings are not available, it is approximated that $D = \beta W_i$ where W_i is the total work done on irreversible processes, measured from the area of the hysteresis loops during fatigue crack

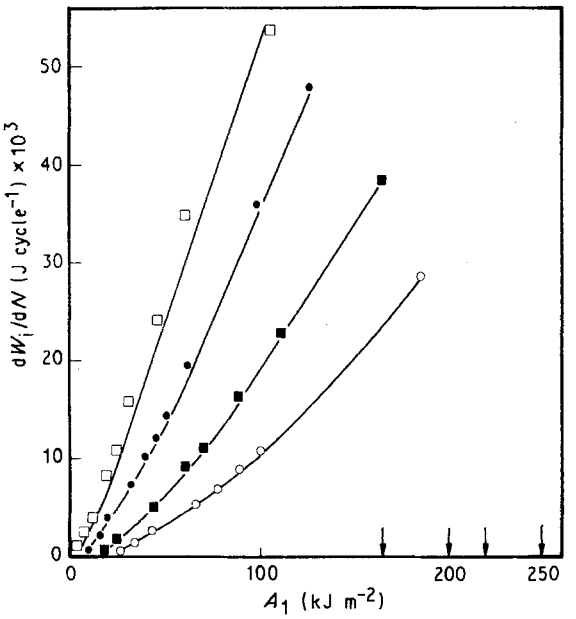

Figure 11 Evolution of energy dissipated per cycle as a function of total energy release rate A_1. Thickness t_0 = (○) 0.33 mm, (■) 0.76 mm, (●) 1.52 mm, (□) 3.22 mm.

growth. Consequently β is the part of W_i that was spent on damage formation. β was found to be equal to unity for these specimens. Representative hysteresis loops for the different thicknesses considered at a crack length of 5 mm are shown in Fig. 10. The evolution of irreversible work expended on damage formation and growth is plotted against the total energy release rate in Fig. 11. With increasing sheet thickness, the rate of energy expenditure on the damage (yielding) process becomes faster.

4.3. Applicability of crack layer theory

All the parameter of Equation 4 are measured independently. The crack speed da/dN is measured from

video recordings of the entire history of crack propagation. W_i is evaluated from the area of the hysteresis loop recorded at prescribed crack lengths. The total energy release rate and the total resistance moments are evaluated from load–displacement curves and active zone configurations [17]. The data points in Fig. 12 represent measurements for different thicknesses and the solid lines correspond to plots of the crack speed on the basis of the crack layer theory.

In the range of sheet thicknesses considered, it can be seen that the crack speeds increase with the sheet thickness at a given A_1. The increase in crack propagation rates with increasing thicknesses observed in PC is in agreement with other reported results [10, 12].

Although the energy required for crack propagation increases with the specimen thickness (Fig. 12), the crack speed is highest with thicker specimens. This is a clear indication that the rate of crack extension is dictated by the level of damage ahead of the crack tip.

Evidently, the proposed formalism provides a good description of the entire range of crack propagation covering more than four orders of magnitude of crack velocity. The well-known S-shaped curve observed in polycarbonate [20] and other materials is described by the proposed formalism. As previously reported, under the experimental conditions considered the phenomenological coefficient β is found to be approximately unity [17].

Since the time of unstable crack propagation (avalanche-like) is negligible, the total lifetime is accounted for by the initiation and propagation of stable cracks.

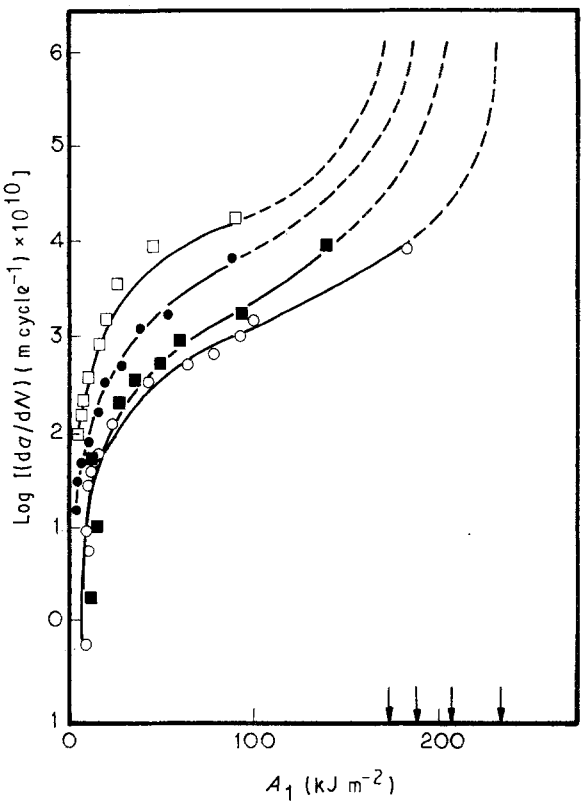

Figure 12 Evolution of crack speed as a function of total energy release rate A_1. The solid lines are the best fit to the crack layer model using $\gamma^* = 60$ J g^{-1}. Thickness $t_0 =$ (○) 0.33 mm, (■) 0.76 mm, (●) 1.52 mm, (□) 3.22 mm.

TABLE I Decomposition of the total number of cycles to fracture for different thicknesses

t (mm)	N_i (cycles)	N_p (cycles)	N_t (cycles)
0.33	8010	1553	9563
0.76	12218	1347	13475
1.52	18543	1094	19637
3.22	27014	838	27852

Accordingly, the total lifetime (in number of cycles) N_t may be expressed as

$$N_t = N_i + N_p \tag{5}$$

where N_i and N_p represent the number of cycles of initiation and propagation, respectively. The effects of thickness on the total lifetime as well as on the time of crack initiation and crack propagation are shown in Table I. Crack initiation is defined as the time required for appearance of a visible crack (~0.2 mm) within the damage zone. Usually the appearance of a crack is associated with an instantaneous change in damage zone geometry. It is seen that the number of cycles for a crack to increase with increase in sheet thickness, while the number of cycles of slow stable crack growth decreases. However, under these experimental conditions the total lifetime of polycarbonate increases with specimen thickness. These results have an importance for practical design application.

4.4. Fracture toughness considerations

Commonly the critical stress intensity factor K_c or the critical energy release rate G_c ($= K_c^2/E$) are considered as material parameters reflecting its resistance to crack propagation, i.e. "fracture toughness". Either is associated with transition from stable (slow) into unstable (uncontrolled) crack propagation. Alternatively a less used critical energy release rate J_{1c} is prescribed as a toughness parameter denoting resistance of the material to initiation of a crack. The crack layer theory, on the other hand, considers fracture as an evolution of an irreversible process, the resistance to which is $\gamma^* R_T$. Accordingly fracture toughness is defined at the transition from stable to unstable crack. This parameter, expressed as A_1, decomposes into a material parameter γ^*, the specific enthalpy of a damage mechanism, and the amount of damage R. Whereas the former is expected to be a constant for a specific type of damage in a material, the latter should reflect the loading history.

A_{1c} decreases rapidly with thickness by more than 40% in the range of thickness considered. Generally, a decrease in the critical energy release rate is associated with brittleness. Nevertheless, it is noted that the mechanism of fracture remains ductile. Obviously, such a parameter is of limited use in characterizing fracture toughness by itself.

As predicted, the amount of damage (yielding) R_{Tc} reflects the stress state imposed by thickness changes. A lesser amount of yielding is observed with increasing thickness. The specific enthalpy of damage

is nearly constant at a value of about 60 J g^{-1}. This is in good agreement with the value reported earlier [17]. The constancy of γ^* found here lends further support to its usefulness as a material parameter, reflecting the intrinsic resistance to crack propagation.

5. Conclusions

1. Fatigue cracks in high molecular weight (M_w = 35 000) Calibre polycarbonate propagate through active zone yielding up to a thickness of 3.22 mm. Above this thickness, a mixed mechanism (yielding and microcracking) is observed.

2. The crack layer formalism has been used to describe crack speed over four decades at thicknesses ranging from 0.33 to 3.22 mm.

3. The critical energy release rate decreases as a function of specimen thickness by more than 40%. A similar decrease is observed in the amount of transformed (yielded) material within the active zone.

4. The specific enthalpy of damage (yielding) is found to be practically constant, independent of thickness. This value is about 60 J g^{-1}.

5. As thickness increases, crack initiation time (as defined in this report) increases while the crack propagation time decreases.

Acknowledgements

The authors wish to acknowledge the financial support of the Dow Chemical Co. and to thank Dr C. P. Bosnyak for stimulating discussions.

References

1. H. F. BRINSON, *Exper. Mech.* **10** (1970) 72.
2. N. WALKER, *Polym. Commun.* **21** (1980) 858.
3. H. HYAKUTAKE and H. NISHITANI, *Eng. Fract. Mech.* **22** (1985) 359.
4. E. H. ANDREWS and S. R. BARNES, in Proceedings of 5th International Conference on Deformation, Yield and Fracture of Polymers, Cambridge, England, March 1982 (The Plastics and Rubber Institute, Cambridge 1982) pp 8. 1–4.
5. A. M. DONALD and E. J. KRAMER, *J. Mater. Sci.* **16** (1981) 2967.
6. *Idem, ibid.* **16** (1981) 2977.
7. J. H. GOLDEN, B. L. HAMMANT and F. A. HAZELL, *J. Appl. Polym. Sci.* **11** (1967) 1571.
8. G. A. ADAM, A. GROSS and R. N. HAWARD, *J. Mater. Sci.* **10** (1975) 1582.
9. M. PARVIN and J. G. WILLIAMS, *Int. J. Fract.* **11** (1975) 963.
10. G. L. PITMAN and I. M. WARD, *Polymer* **15** (1980) 635.
11. G. C. MARTIN and W. W. GERBERICH, *J. Mater. Sci.* **11** (1976) 231.
12. G. L. PITMAN and I. M. WARD, *Polymer* **20** (1979) 895.
13. S. ARAD, J. C. RADON and L. W. CULVER, *J. Appl. Polym. Sci.* **17** (1973) 1467.
14. J. A. MANSON and R. W. HERTZBERG, *CRC Rev. Macromol. Sci.* **1** (1973) 433.
15. M. T. TAKEMORI and R. P. KAMBOUR, *J. Mater. Sci.* **16** (1981) 1108.
16. M. KITAGAWA, *J. Mater. Sci.* **17** (1982) 2514.
17. N. HADDAOUI, A. CHUDNOVSKY and A. MOET, *Polymer* **27** (1986) 1378.
18. J. F. KNOTT, "Fundamentals of Fracture Mechanics" (Butterworths, London, 1973) pp 86–8.
19. A. CHUDNOVSKY, "The Crack Layer Theory", NASA Report No. 174 134 (Case Western Reserve University, 1984).
20. S. ARAD, J. C. RADON and L. E. CULVER, *J. Mater. Sci.* **13** (1971) 75.

Received 10 March
and accepted 30 June 1992